

Nonlinear transmission and light localization in photonic crystal waveguides

Sergei F. Mingaleev and Yuri S. Kivshar

*Nonlinear Physics Group, Research School of Physical Sciences and Engineering
Australian National University, Canberra ACT 0200, Australia*

We study the light transmission in two-dimensional photonic crystal waveguides with embedded nonlinear defects. First, we derive the effective discrete equations with long-range interaction for describing the waveguide modes, and demonstrate that they provide a highly accurate generalization of the familiar tight-binding models which are employed, e.g., for the study of the coupled-resonator optical waveguides. Using these equations, we investigate the properties of straight waveguides and waveguide bends with embedded nonlinear defects and demonstrate the possibility of the nonlinearity-induced bistable transmission. Additionally, we study localized modes in the waveguide bends and (linear and nonlinear) transmission of the bent waveguides and emphasize the role of evanescent modes in these phenomena.

1. Introduction

Photonic crystals are usually viewed as an optical analog of semiconductors that modify the properties of light similar to a microscopic atomic lattice that creates a semiconductor band-gap for electrons¹. One of the most promising applications of photonic crystals is a possibility to create compact integrated optical devices², which would be analogous to the integrated circuits in electronics, but operating entirely with light. Replacing relatively slow electrons with photons as the carriers of information, the speed and bandwidth of advanced communication systems can be dramatically increased, thus revolutionizing the telecommunication industry.

To employ the high-tech potential of photonic crystals for optical applications and all-optical switching and waveguiding technologies, it is crucially important to achieve a dynamical tunability of their properties. For this purpose, several approaches have been suggested (see, e.g., Ref. 3). One of the most promising concepts is based on the idea to employ the properties of *nonlinear photonic crystals*, i.e. photonic crystals made from dielectric materials whose refractive index depends on the light intensity. Exploration of nonlinear properties of photonic band-gap materials is an important direction of current research that opens a broad range of novel applications of photonic crystals for all-optical signal processing and switching, allowing an effective way to create highly tunable band-gap structures operating entirely with light.

One of the important concepts in the physics of photonic crystals is related to the field localization on defects. In the solid-state physics, the idea of localization is associated with disorder that breaks the translational

invariance of a crystal lattice and supports spatially localized modes with the frequency outside the phonon bands. The similar concept is well-known in the physics of photonic crystals where an isolated defect (a region with different refractive index which breaks periodicity) is known to support a localized defect mode. An array of such defects creates a waveguide that allows a directed light transmission for the frequencies inside the band gap. Since the frequencies of the defect modes created by *nonlinear defects* depend on the electric field intensity, such modes can be useful to control the light transmission. From the viewpoint of possible practical applications, spatially localized states in optics can be associated with different types of all-optical switching devices where light manipulates and controls light itself due to the varying input intensity.

Nonlinear photonic crystals and photonic crystals with embedded nonlinear defects create an ideal environment for the observation of many of the nonlinear effects earlier predicted and studied in other branches of physics. In particular, the existence of nonlinear localized modes with the frequencies in the photonic band gaps has already been predicted and demonstrated numerically for several models of photonic crystals with the Kerr-type nonlinearity^{4–6}.

In this paper, we study the resonant light transmission and localization in the photonic crystal waveguides and bends with embedded nonlinear defects. For simplicity, we consider the case of a photonic crystal created by a square lattice of infinite dielectric rods, with waveguides made by removing some of the rods. Nonlinear properties of the waveguides are controlled by embedding the nonlinear defect rods. We demonstrate that the effective interaction in such waveguiding structures

is nonlocal, and we suggest a novel theoretical approach, based on the effective discrete equations, for describing both linear and nonlinear properties of such photonic-crystal waveguides and circuits, including the localized states at the waveguide bends. Additionally, we study the transmission of waveguide bends and emphasize the role of evanescent modes for the correct analysis of their properties.

The paper is organized as follows. In Sec. 2, we introduce our model of a two-dimensional (2D) photonic crystal and provide a brief derivation of the effective discrete equations for the photonic-crystal waveguides created by removed or embedded rods, based on the Green function technique. In Sec. 3, we apply these discrete equations for the analysis of the transmission of straight waveguides, including the resonant transmission through an array of nonlinear defect rods embedded into a straight waveguide. Additionally, we discuss a link between our approach and the results obtained in the framework of the familiar tight-binding approximation often used in the solid-state physics models, and emphasize the important role of the evanescent modes which can not be accounted for in the framework of the tight-binding approximation. Section 4 is devoted to the study of waveguide bends. First, we discuss the localized modes supported by a waveguide bend, and then we analyze the transmission of the waveguide bends. We demonstrate that the waveguide bends with embedded nonlinear defects can be used for a very effective control of light transmission. Section 5 concludes the paper with a summary of the results and further applications of our approach.

2. Effective discrete equations

In this Section, we suggest and describe a novel theoretical approach, based on the effective discrete equations, for describing many of the properties of the photonic-crystal waveguides and circuits, including the transmission spectra of sharp waveguide bends. This is *an important part of our analysis* because the properties of the photonic crystals and photonic crystal waveguides are usually studied by solving Maxwell's equations numerically, and such calculations are, generally speaking, time consuming. Moreover, the numerical solutions do not always provide a good physical insight. The effective discrete equations we derive below and employ further in the paper are somewhat analogous to the Kirchhoff equations for the electric circuits. However, in contrast to electronics, in photonic crystals both diffraction and interference become important, and thus the resulting equations involve the long-range interaction effects.

We introduce our approach for a simple model of 2D photonic crystals consisting of infinitely long dielectric rods arranged in the form of a square lattice with the lattice spacing a . We study the light propagation in the plane normal to the rods, assuming that the rods have a

radius $r_0 = 0.18a$ and the dielectric constant $\varepsilon_0 = 11.56$ (this corresponds to GaAs or Si at the wavelength $\sim 1.55 \mu\text{m}$). For the electric field $E(\vec{x}, t) = e^{-i\omega t} E(\vec{x}|\omega)$ polarized parallel to the rods, Maxwell's equations reduce to the eigenvalue problem

$$\left[\nabla^2 + \left(\frac{\omega}{c} \right)^2 \varepsilon(\vec{x}) \right] E(\vec{x}|\omega) = 0, \quad (1)$$

which can be solved by the plane-wave method⁷. A perfect photonic crystal of this type possesses a large (38%) complete band gap between $\omega = 0.303 \times 2\pi c/a$ and $\omega = 0.444 \times 2\pi c/a$ (see Fig. 1), and it has been extensively employed during last few years for the study of bound states⁸, transmission of light through sharp bends^{9,10}, waveguide branches¹¹ and intersections¹², channel drop filters¹³, nonlinear localized modes in straight waveguides⁵ and discrete spatial solitons in perfect 2D photonic crystals⁶. Recently, this type of photonic crystal with a 90° bent waveguide has been fabricated in macro-porous silicon with $a = 0.57 \mu\text{m}$ and a complete band gap at $1.55 \mu\text{m}$ ¹⁴.

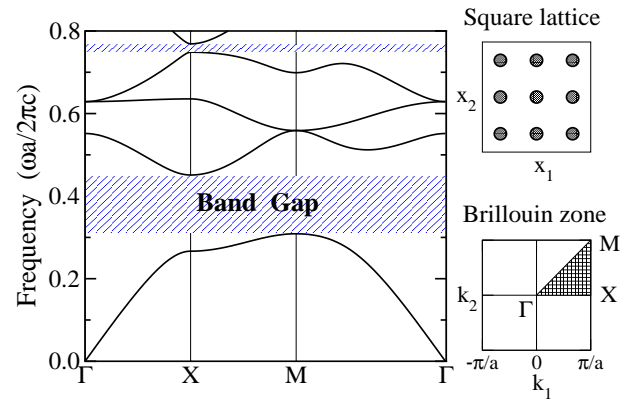


Fig. 1. The band-gap structure of the photonic crystal created by a square lattice of dielectric rods with $r_0 = 0.18a$ and $\varepsilon_0 = 11.56$; the band gaps are hatched. The top right inset shows a cross-sectional view of the 2D photonic crystal. The bottom right inset shows the corresponding Brillouin zone, with the irreducible zone shaded.

To create a waveguide circuit, we introduce a system of defects and assume, for simplicity, that the defects are identical rods of the radius r_d located at the points \vec{x}_n , where n is the index number of the defect rods. Importantly, the similar approach can be employed equally well for the study of the defects created by removing isolated rods in a perfect 2D lattice, and we demonstrate such examples below.

In the photonic crystal with defects, the dielectric constant $\varepsilon(\vec{x})$ can be presented as a sum of the periodic and defect-induced terms, i.e. $\varepsilon(\vec{x}) = \varepsilon_p(\vec{x}) + \delta\varepsilon(\vec{x})$, with

$$\delta\varepsilon(\vec{x}) = \sum_n \varepsilon_d [E(\vec{x}|\omega)] f(\vec{x} - \vec{x}_n), \quad (2)$$

where $f(\vec{x}) = 1$ for $|\vec{x}| < r_d$, and it vanishes otherwise.

Equation (1) can be therefore written in the following integral form

$$E(\vec{x}|\omega) = \left(\frac{\omega}{c}\right)^2 \int d^2\vec{y} \, G(\vec{x}, \vec{y}|\omega) \delta\varepsilon(\vec{y}) E(\vec{y}|\omega), \quad (3)$$

where $G(\vec{x}, \vec{y}|\omega)$ is the Green function of a perfect 2D photonic crystal (see, e.g., Ref. 5).

A single defect rod is described by the function $\delta\varepsilon(\vec{x}) = \varepsilon_d f(\vec{x})$, and it can support one or more localized modes. Such localized modes are the eigenmodes of the discrete spectrum of the following eigenvalue problem,

$$\mathcal{E}_l(\vec{x}) = \left(\frac{\omega_l}{c}\right)^2 \int_{r_d} d^2\vec{y} \, G(\vec{x}, \vec{y}|\omega_l) \varepsilon_d f(\vec{y}) \mathcal{E}_l(\vec{y}), \quad (4)$$

where ω_l is the frequency (a discrete eigenvalue) of the l -th eigenmode and $\mathcal{E}_l(\vec{x})$ is the corresponding electric field.

When we increase the number of defect rods (for example, in order to create photonic-crystal waveguide circuits^{9–13}), the numerical solution of the integral equation (3) becomes complicated and, moreover, it is severely restricted by the current computer facilities. Therefore, one of our major goals in this paper is to develop a new approximate physical model that would allow the application of fast numerical techniques, combined with a reasonably good accuracy, for the study of more complicated (linear and nonlinear) waveguide circuits in photonic crystals.

To achieve our goal, we consider the localized states created by a (in general, complex) system of defects (2) as a linear combination of the localized modes $\mathcal{E}_l(\vec{x})$ supported by isolated defects:

$$E(\vec{x}|\omega) = \sum_{l,n} \psi_n^{(l)}(\omega) \mathcal{E}_l(\vec{x} - \vec{x}_n). \quad (5)$$

Substituting Eq. (5) into Eq. (3), multiplying it by $\mathcal{E}_{l'}(\vec{x} - \vec{x}_{n'})$ and integrating with \vec{x} , we obtain a system of discrete equations for the amplitudes $\psi_n^{(l)}$ of the l -th eigenmodes localized at n -th defect rods:

$$\sum_{l,n} \lambda_{l,n}^{l',n'} \psi_n^{(l)} = \sum_{l,n,m} \varepsilon_d \mu_{l,n,m}^{l',n'}(\omega) \psi_n^{(l)}, \quad (6)$$

where

$$\begin{aligned} \lambda_{l,n}^{l',n'} &= \int d^2\vec{x} \, \mathcal{E}_l(\vec{x} - \vec{x}_n) \mathcal{E}_{l'}(\vec{x} - \vec{x}_{n'}), \\ \mu_{l,n,m}^{l',n'}(\omega) &= \left(\frac{\omega}{c}\right)^2 \int d^2\vec{x} \, \mathcal{E}_{l'}(\vec{x} - \vec{x}_{n'}) \times \\ &\quad \int d^2\vec{y} \, G(\vec{x}, \vec{y}|\omega) f(\vec{y} - \vec{x}_m) \mathcal{E}_l(\vec{y} - \vec{x}_n). \end{aligned} \quad (7)$$

It should be emphasized that the discrete equations (6)–(7) are derived by using only the approximation provided by the ansatz (5). As can be demonstrated by comparing the approximate results with the direct numerical solutions of the Maxwell equations, this approximation is usually very accurate, and it can be used in many physical problems.

However, the effective discrete equations (6) are still too complicated and, in some cases, they can be simplified further still remaining very accurate. A good example is the case of the photonic crystal waveguides created by a sequence of largely separated defect rods. Such waveguides are known as *the coupled-resonator optical waveguides* (CROWs)^{15,16} or *coupled-cavity waveguides* (CCWs)¹⁷. For those cases, the localized modes are located at each of the defect sites being only weakly coupled with the similar neighboring modes. As is known, such a situation can be described very accurately by the so-called *tight-binding approximation* (see also Ref. 18). For our formalism, this means that $\lambda_{l,n}^{l',n'} = \mu_{l,n,m}^{l',n'} = 0$ for $|n' - n| > 1$ and $|n' - m| > 1$. The most important feature of the CROW circuits is that their bends are reflectionless throughout the entire band^{15,17}. This is in a sharp contrast with the conventional photonic crystal waveguides created by a sequence of the removed or introduced defect rods (see e.g., Ref. 9 and references therein) where the 100% transmission through a waveguide bend is known to occur only at certain resonant frequencies. In spite of this visible advantage, the CROW structures have a very narrow guiding band and, as a result, effectively they demonstrate a complete transmission through the waveguide bend in a narrow frequency interval too.

Below, we consider different types of photonic crystal waveguides and show that a very accurate simplification of Eqs. (6) is provided by accounting for *an indirect coupling* between the remote defect modes, caused by the slowly decaying Green function, $\mu_{l,n,m}^{l',n'} \neq 0$ for $|n' - n| \leq L$, where the number L of effectively coupled defects lies usually between five and ten. As we show below, this type of interaction, which is neglected in the tight-binding approximation, is important for understanding the transmission properties of the photonic-crystal waveguides. At the same time, we neglect a direct overlap between the nearest-neighbor eigenmodes, which is often considered to be important^{15,17}), i.e. we consider $\lambda_{l,n}^{l',n'} = \delta_{l,l'} \delta_{n,n'}$ (with $\delta_{l,l'}$ being the Dirac delta function) and $\mu_{l,n,m}^{l',n'} = 0$ for $n \neq m$. Taking into account this interaction leads to negligible corrections only.

Assuming that the defects support only *the monopole eigenmodes* (marked by $l = 1$), the coefficients (7) can be calculated reasonably accurately in approximation that the electric field remains constant inside the defect rods, i.e. $\mathcal{E}_1(\vec{x}) \sim f(\vec{x})$. This corresponds to the averaging of the electric field in the integral equation (3) over the cross-section of the defect rods^{19,5}. In this case the re-

sulting approximate discrete equation for the amplitudes of the electric fields $E_n(\omega) \equiv \psi_n^1(\omega)$ of the eigenmodes excited at the defect sites has the following matrix form:

$$\sum_m M_{n,m}(\omega) E_m(\omega) = 0, \quad (8)$$

$$M_{n,m}(\omega) = \varepsilon_d(E_m) J_{n,m}(\omega) - \delta_{n,m},$$

where $J_{n,m}(\omega) \equiv \mu_{1,m,n}^{1,n}(\omega)$ is a coupling constant calculated in the approximation that $\mathcal{E}_1(\vec{x}) \sim f(\vec{x})$, so that

$$J_{n,m}(\omega) = \left(\frac{\omega}{c}\right)^2 \int_{r_d} d^2\vec{y} G(\vec{x}_n, \vec{x}_m + \vec{y} | \omega) \quad (9)$$

is completely determined by the Green function of a perfect 2D photonic crystal (see details in Refs. 5,6).

First of all, we check the accuracy of our approximate model (8) for the case of a *single defect* located at the point \vec{x}_0 . In this case, Eq. (8) yields the simple result $J_{0,0}(\omega_d) = 1/\varepsilon_d$, and this expression defines the frequency ω_d of the defect mode. In particular, applying this result to the case when the defect is created by a single removed rod, we obtain the frequency $\omega_d = 0.391 \times 2\pi c/a$ which differs only by 1% from the value $\omega_d = 0.387 \times 2\pi c/a$ calculated with the help of the MIT Photonic-Bands numerical code⁷.

3. Straight waveguides

A. Waveguide dispersion

A simple single-mode waveguide can be created by removing a row of rods (see the inset in Fig. 2). Assuming that the waveguide is straight ($M_{n,m} \equiv M_{n-m}$) and neglecting the coupling between the remote defect rods (i.e. $M_{n-m} = 0$ for all $|n-m| > L$), we rewrite Eq. (8) in the transfer-matrix form, $\vec{F}_{n+1} = \hat{T} \vec{F}_n$, where we introduce the vector $\vec{F}_n = \{E_n, E_{n-1}, \dots, E_{n-2L+1}\}$ and the transfer matrix $\hat{T} = \{T_{i,j}\}$ with the non-zero elements

$$T_{1,j}(\omega) = -\frac{M_{L-j}(\omega)}{M_L(\omega)} \quad \text{for } j = 1, 2, \dots, 2L,$$

$$T_{j,j+1} = 1 \quad \text{for } j = 1, 2, \dots, 2L-1. \quad (10)$$

Solving the eigenvalue problem

$$\hat{T}(\omega) \vec{\Phi}^p = \exp\{ik_p(\omega)\} \vec{\Phi}^p, \quad (11)$$

we can find the $2L$ eigenmodes of the photonic-crystal waveguide. The eigenmodes with real wavenumbers $k_p(\omega)$ correspond to the modes propagating along the waveguide. In the waveguide shown in Fig. 2, there exist only two such modes (we denote them as $\vec{\Phi}^1$ and $\vec{\Phi}^2$), propagating in the opposite directions ($k_1 = -k_2 > 0$).

In Fig. 2 we plot the dispersion relation $k_1(\omega)$ calculated by *three different methods*: first (solid curve) is calculated directly by the super-cell method⁷, and other two are found from Eq. (11) in the nearest-neighbor approximation ($L=1$, dotted curve) corresponding to the tight-binding models, and also by taking into account the long-range interaction through the coupling between several neighbors ($L=7$, dashed curve). Indeed, we observe a very good agreement for the conditions when the long-range interaction is taken into account.

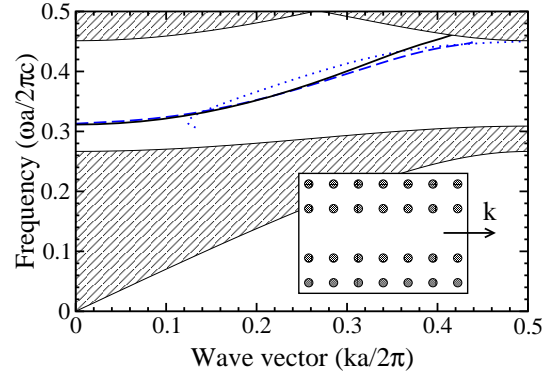


Fig. 2. Dispersion relation for a 2D photonic-crystal waveguide (shown in the inset) calculated by the super-cell method⁷ (solid), and from the approximate equations (10)–(11) for $L=7$ (dashed) and $L=1$ (dotted). The hatched areas are the projected band structure of a perfect 2D crystal.

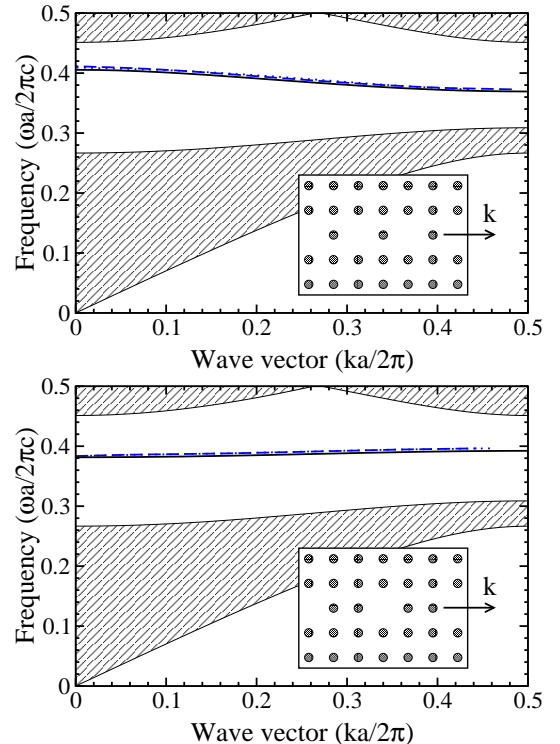


Fig. 3. The same as in Fig. 2 but for two other types of waveguides better described by the tight-binding models.

It is important to compare the results provided by our method with those obtained in the tight-binding approximation. For the waveguide shown in Fig. 2, such an approximation, rigorously speaking, is not valid, but its analog can be considered at least formally for the case of the nearest-neighbor interaction when in Eqs. (10)–(11) we take $L=1$. The interaction between the remote rods cannot be neglected as soon as we study the waveguides created by removing (or inserting) all rods along the row or more complicated structures of this type. In such a case, as is seen from Fig. 2, the dispersion relation found in the tight-binding approximation is incorrect and, in order to obtain accurate results, one should take into account the coupling between several defect rods. We verify that this statement is also valid for multi-mode waveguides, e.g. those created by removing several rows of rods.

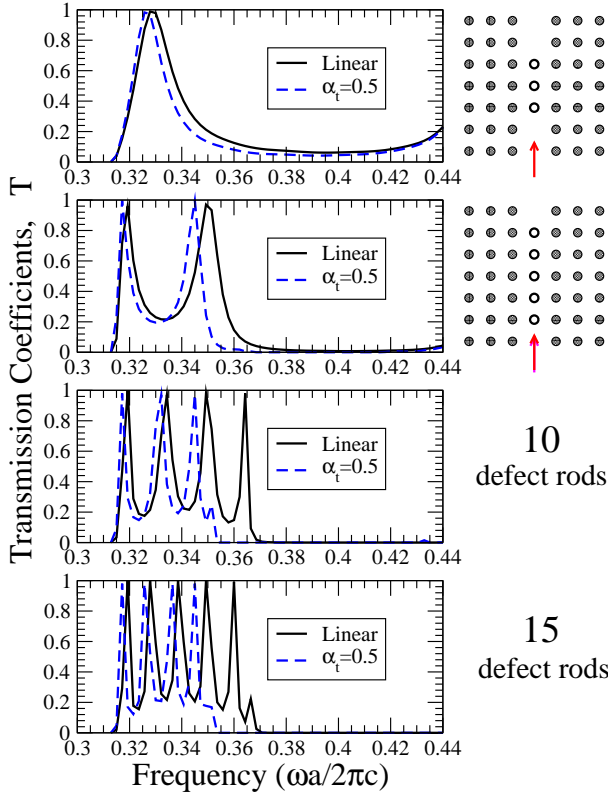


Fig. 4. Transmission coefficients of an array of nonlinear defect rods calculated from Eqs. (8)–(13) with $L = 7$ in the linear limit of very small $|\alpha_t|^2$ (solid curves) and for the nonlinear transmission when the output intensity is $|\alpha_t|^2 = 0.25$ (dashed curves), for different numbers of the defects. We use nonlinear defect rods with the dielectric constant $\epsilon_d^{(0)} = 7$; they are marked by open circles on the right insets.

However, for the waveguides of a different geometry, when only the second (or third, etc) rods are removed, all methods provide a reasonably good agreement with the direct numerical results, as is shown for two examples in Fig. 3. In this case, the waveguides are created by an array of cavity modes, and they are simi-

lar to the CROW structures earlier analyzed by several authors^{15–17}. Thus, the dispersion properties of CROWs (or similar waveguides) can be described with a good accuracy by the tight-binding approximation; our new approach confirms this conclusion, and it provides a simple method for the derivation of the approximate equations.

B. Resonant transmission of an array of defects

In addition to the propagating guided modes, in photonic crystal waveguides there always exist *evanescent modes* with imaginary k_p . These modes cannot be accounted for in the framework of the tight-binding theory that relies on the nearest-neighbor interaction between the defect rods. Although the evanescent modes remain somewhat “hidden” in straight waveguides, they become crucially important in more elaborated structures such as waveguides with embedded linear or nonlinear defects, waveguide bends and branches. In these cases the evanescent modes manifest themselves in several different ways. In particular, they determine *non-trivial transmission properties* of the photonic-crystal circuits considered below.

As the first example of the application of our approach, we study the transmission of a straight waveguide with embedded nonlinear defects. Such a structure can be considered as two semi-infinite straight waveguides coupled by a finite region of defects located between them. The coupling region may include both linear (as a domain of a perfect waveguide) and nonlinear (embedded) defects. We assume that the defect rods inside the coupling region are characterized by the index that runs from a to b , and the amplitudes E_m ($m = a, \dots, b$) of the electric field at the defects are all unknown. We number the guided modes (11) in the following way: $p = 1$ corresponds to the mode propagating in the direction of the nonlinear section (for both ends of the waveguide), $p = 2$ corresponds to the mode, propagating in the opposite direction, $p = 3, \dots, L + 1$ correspond to the evanescent modes which grow in the direction of the nonlinear section, and $p = L + 2, \dots, 2L$ correspond to the evanescent modes which decay in the direction of the nonlinear section. Then, we can write the incoming and outgoing waves in the semi-infinite waveguide sections as a superposition of the guided modes:

$$E_m^{in} = \alpha_i \Phi_{a-m}^1 + \alpha_r \Phi_{a-m}^2 + \sum_{p=3}^{L+1} \beta_p^{in} \Phi_{a-m}^p, \quad (12)$$

for $m = a - 2L, \dots, a - 1$, and

$$E_m^{out} = \alpha_t \Phi_{m-b}^2 + \sum_{p=3}^{L+1} \beta_p^{out} \Phi_{m-b}^p, \quad (13)$$

for $m = b + 1, \dots, b + 2L$, where β_p^{in} and β_p^{out} are unknown amplitudes of the evanescent modes growing in the direction of the nonlinear section, whereas α_i , α_t and α_r ,

are unknown amplitudes of the incoming, transmitted, and reflected propagating waves. We take into account that the evanescent modes with $p > L + 1$ (growing in the direction of waveguide ends) must vanish. Now, substituting Eqs. (12)–(13) into Eq. (8), we obtain a system of linear (or nonlinear, for nonlinear defects) equations with $2L + b - a + 1$ unknown. Solving this system, we find the transmission coefficient, $T = |\alpha_t/\alpha_i|^2$, and reflection coefficient, $R = |\alpha_r/\alpha_i|^2$, as functions of the light frequency, ω , and intensity, $|\alpha_i|^2$ or $|\alpha_t|^2$. Recently, we have demonstrated²⁰ that the linear transmission properties of the waveguide bends are described very accurately by this approach. Below, we study *nonlinear transmission* of the photonic-crystal waveguides and waveguide bends.

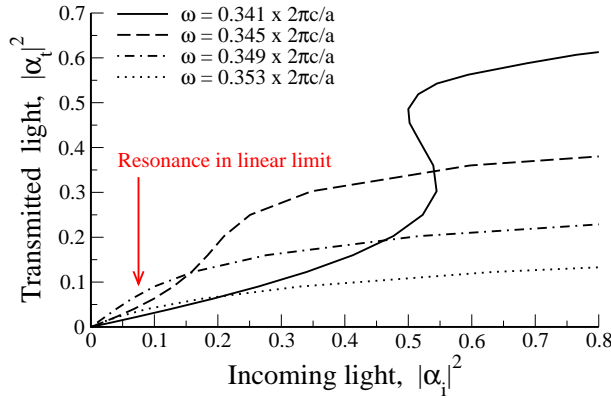


Fig. 5. Bistability in the nonlinear transmission of an array of five nonlinear defect rods shown in Fig. 4(b).

In Fig. 4, we present our results for the transmission spectra of the straight waveguides (created by a row of removed rods) with an array of embedded nonlinear defects. We assume throughout the paper that all nonlinear defect rods are identical, with the radius $r_d = r_0 = 0.18a$ and the dielectric constant, $\varepsilon_d = \varepsilon_d^{(0)} + |E_n|^2$ (with $\varepsilon_d^{(0)} = 7$), which grows linearly with the light intensity (the so-called Kerr effect). In the linear limit, the embedded defects behave like an effective resonant filter, and only the waves with some specific resonance frequencies can be effectively transmitted through the defect section. The resonances appear due to the excitation of cavity modes inside the defect region, whereas a single defect does not demonstrate any resonant behavior. When the intensity of the input wave grows, the resonant frequencies found in the linear limit get shifted to lower values. The sensitivity of different resonances to the change of the light intensity is quite different and may be tuned by matching of the defect parameters. The nonlinear resonant transmission is found to possess *bistability*, similar to another problem of the nonlinear transmission (see, e.g., Refs. 21). The bistable transmission occurs for the frequencies smaller than the resonant, in a linear limit, frequency (see Fig. 5).

C. An optical diode

An all-optical “diode” is a spatially nonreciprocal device which allows unidirectional propagation of a signal at a given wavelength. In the ideal case, the diode transmission is 100% in the “forward” propagation, while it is much smaller or vanishes for “backward” (opposite) propagation, yielding a unitary contrast.

The first study of the operational mechanism for a passive optical diode based on a photonic band gap material was carried out by Scalora *et al.*^{22,23}. These authors considered the pulse propagation near the band edge of a one-dimensional photonic crystal structure with a spatial gradation in the linear refractive index, together with a nonlinear medium response, and found that such a structure can result in unidirectional pulse propagation.

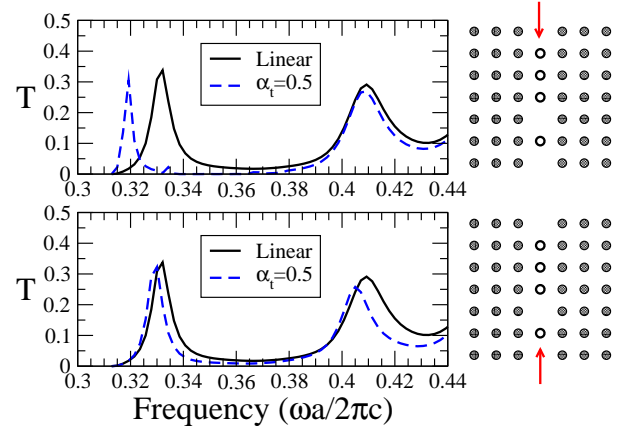


Fig. 6. Transmission coefficients of an asymmetric array of nonlinear defect rods calculated for the same parameters as in Fig. 4.

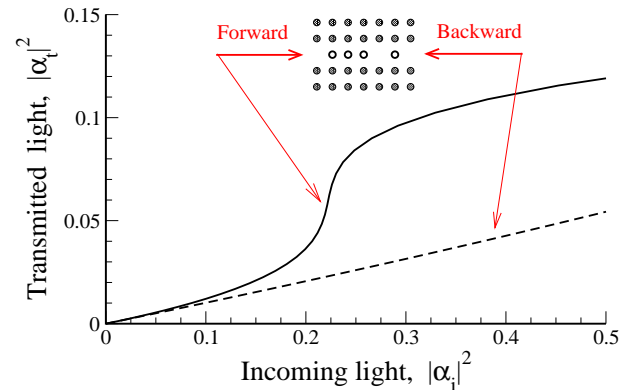


Fig. 7. Nonlinear transmission of the optical diode for the forward (see top of Fig. 6) and backward (see bottom of Fig. 6) directions at the light frequency $\omega = 0.326 \times 2\pi c/a$.

To implement this concept for the waveguide geometry discussed above, we consider the asymmetric structure made of four nonlinear defect rods, as shown in the right insets on Fig. 6. Figure 6 shows the transmission spectra

of such an asymmetric structure in the opposite directions indicated by two arrows in the right insets. As is seen, in the linear limit the transmission is characterized by two resonant frequencies and does not depend on the propagation direction. However, since the sensitivity of both resonant frequencies to the change of the light intensity is different for the “forward” (see Fig. 6, top) and “backward” (see Fig. 6, bottom) propagation directions, the transmission becomes, in the vicinity of resonant frequencies, highly asymmetric for large input intensities. This results into nearly unidirectional waveguide transmission, as shown in Fig. 7.

In contrast to the perfect resonators used in Fig. 4, the transmission of the asymmetric structure under consideration is not very efficient at the resonant frequencies. However, we believe that the optical diode effect, with much better efficiency, can be found in other types of the waveguide geometry and a unitary contrast can be achieved by a proper optimization of the waveguide and defect parameters, that can be carried out by employing our method and the effective discrete equations derived above.

4. Waveguide bends

In addition to the non-trivial transmission properties, the evanescent modes manifest themselves in creation of *localized bound states* in the vicinity of the waveguide bends or branches. To demonstrate this effect, we consider the simplest case of a sharp bend of the waveguide created by a row of removed rods. As was shown in Ref. 8, in the cases when the waveguide bend can be considered as a finite section of a waveguide of different type, the bound states correspond closely to cavity modes excited in this finite section. However, such a simplified one-dimensional model does not describe correctly more complicated cases⁸, even the properties of the bent waveguide depicted in Fig. 8. The situation becomes even more complicated for the waveguide branches¹¹. In contrast, solving the discrete equations (8) we can find the frequencies and profiles of the bound states excited in an arbitrary complex set of defects. For particular case of the waveguide bend shown in Fig. 8, we find two bound states localized at the bend and their profiles (cf. our Fig. 8 with Fig. 9 in Ref. 8). It should be noted that the frequencies of the modes are found from Eq. (8) with the accuracy of 1.5%.

Additionally, the evanescent modes determine the non-trivial transmission properties of the waveguide bends which can also be calculated with the help of our discrete equations. To demonstrate these features, we consider a bent waveguide consisting of two coupled semi-infinite straight waveguides with a finite section of defects between them. The finite section includes a bend with a safety margin of the straight waveguide at both ends.

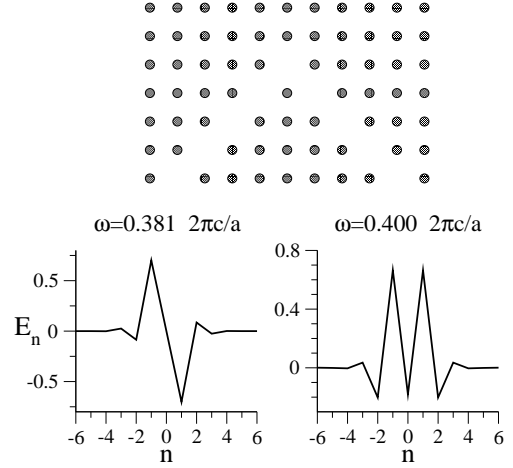


Fig. 8. Electric field E_n for two bound states supported by a 90° waveguide bend shown in the top. Center of the bend is located at $n = 0$.

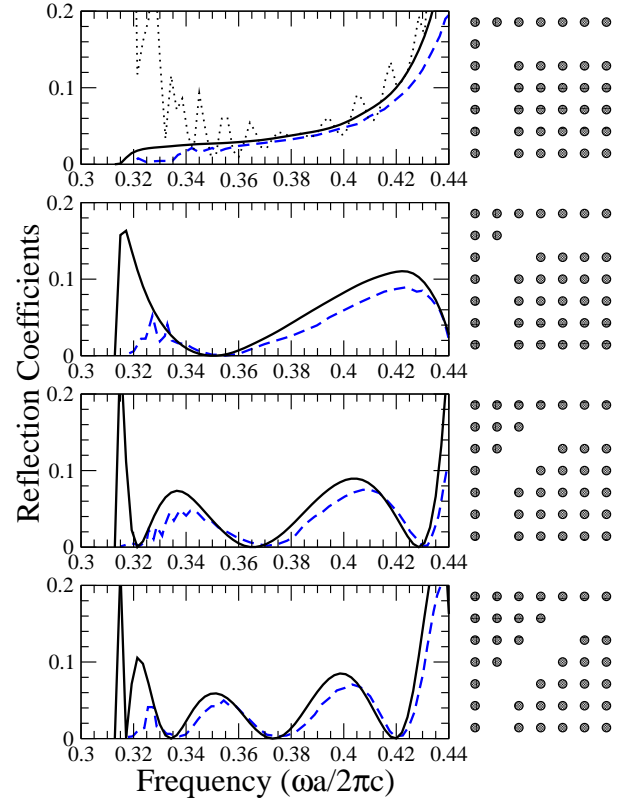


Fig. 9. Reflection coefficients calculated by the finite-difference time-domain method (dashed, from Ref. 9) and from Eqs. (8)–(13) with $L = 7$ (full lines) and $L = 2$ (dotted, only in the top plot), for different bend geometries.

Similar to what we discussed in Sec. 3B for the straight waveguides, we solve the system of effective discrete equations to find the transmission, $T = |\alpha_t/\alpha_i|^2$, and reflection, $R = |\alpha_r/\alpha_i|^2$, coefficients of the waveguide bends. In Fig. 9 we present our results for the transmission spectra of several types of bent waveguides,

which have been discussed in Ref. 9, where the possibility of high transmission through sharp bends in photonic-crystal waveguides was first demonstrated. We compare the reflection coefficients calculated by the finite-difference time-domain method in Ref. 9 (dashed lines) with our results, calculated from Eqs. (8)–(13) for $L = 7$ (full lines) and for $L = 2$ (dotted line in the top plot). As is clearly seen, Eqs. (8)–(13) provide a very accurate method for calculating the transmission spectra of the waveguide bends, if only we account for long-range interactions. It should be emphasized that the approximation, in which the only next-neighbor interactions are taken in to account, is usually too crude, while the tight-binding theory incorrectly predicts a perfect transmission for all guiding frequencies.

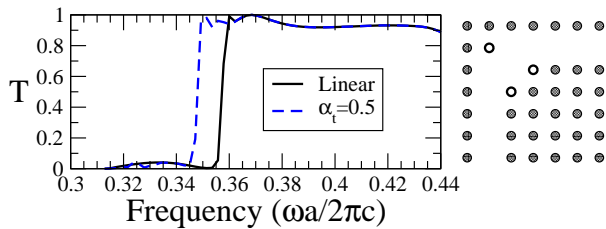


Fig. 10. Transmission of a waveguide bend with three embedded nonlinear defect rods in the linear (solid curve) and nonlinear (dashed curve) regimes. Defect rods have the dielectric constant $\epsilon_d^{(0)} = 7$, and they are marked by open circles.

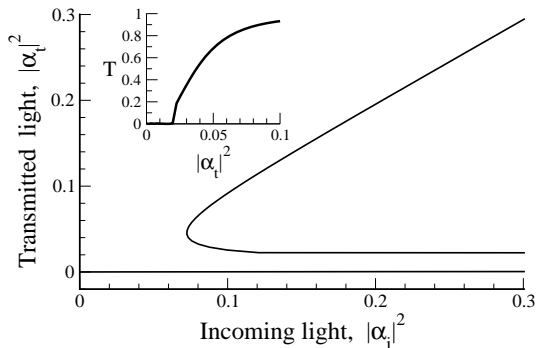


Fig. 11. Bistable nonlinear transmission through the waveguide bend shown in Fig. 10, for the light frequency $\omega = 0.351 \times 2\pi c/a$.

The resonant transmission can be modified dramatically by introducing both linear and/or nonlinear defects into the waveguide bends. To illustrate such features, we consider the waveguide bend with three embedded nonlinear defects, as is depicted in Fig. 10 on the right inset, where these defects are shown by open circles. In the linear regime, such a sharp bend behaves as an optical threshold device that efficiently transmits the guided waves with frequencies above the threshold one, but completely reflects the waves with the lower frequencies. The transmission coefficient of this waveguide bend in the linear limit is shown in Fig. 10 by a solid

curve. When the input intensity increases, the threshold frequency decreases, extending the transmission region (see a dashed curve in Fig. 10). The resulting transmission as a function of the input intensity demonstrates a sharp nonlinear threshold character with an extremely low transmission of the waves below a certain (rather small) threshold intensity, see Fig. 11.

5. Conclusions

We have suggested a novel theoretical approach for describing a broad range of transmission properties of the photonic crystal waveguides and circuits. Our approach is based on the analysis of the effective discrete equations derived with the help of the Green function technique, and it generalizes the familiar tight-binding approximations usually employed to study the coupled-resonator or coupled-cavity optical waveguides. The effective discrete equations we have introduced in this paper emphasize the important role played by the evanescent modes in the transmission characteristics of the photonic crystal circuits with waveguide bends and/or embedded defects. Employing this technique, we have studied the properties of several important elements of the (linear and nonlinear) photonic crystal circuits, including a nonlinear bistable transmitter and an optical diode created by an asymmetric structure of nonlinear defects. We believe that our approach can be useful for solving more complicated problems, and it can be applied to study the transmission characteristics of the waveguide branches, channel drop filters, etc.

The work has been partially supported by the Australian Research Council.

1. J. D. Joannopoulos, R. B. Meade, and J. N. Winn, *Photonic Crystals: Molding the Flow of Light* (Princeton University Press, Princeton N.J., 1995).
2. K. Sakoda, *Optical Properties of Photonic Crystals* (Springer-Verlag, Berlin, 2001); see also a comprehensive review paper, T.F. Krauss and R.M. De la Rue, “Photonic crystals in the optical regime—past, present and future”, *Prog. Quantum Electron.* **23**, 51-96 (1999), and references therein.
3. See, e.g., K. Busch and S. John, “Liquid-crystal photonic-band-gap materials: The tunable electromagnetic vacuum”, *Phys. Rev. Lett.* **83**, 967-970 (1999), and discussions therein.
4. S. John and N. Aközbek, “Nonlinear optical solitary waves in a photonic band gap”, *Phys. Rev. Lett.* **71**, 1168-1171 (1993); “Optical solitary waves in two- and three-dimensional nonlinear photonic band-gap structures”, *Phys. Rev. E* **57**, 2287-2319 (1998).

5. S.F. Mingaleev, Yu.S. Kivshar, and R.A. Sammut, "Long-range interaction and nonlinear localized modes in photonic crystal waveguides", *Phys. Rev. E* **62**, 5777-5782 (2000).
6. S.F. Mingaleev and Yu.S. Kivshar, "Self-trapping and stable localized modes in nonlinear photonic crystals", *Phys. Rev. Lett.* **86**, 5474-5477 (2001).
7. S.G. Johnson and J.D. Joannopoulos, "Block-iterative frequency-domain methods for Maxwell's equations in a planewave basis", *Optics Express* **8**, 173-190 (2001).
8. A. Mekis, S.H. Fan, and J.D. Joannopoulos, "Bound states in photonic crystal waveguides and waveguide bends", *Phys. Rev. B* **58**, 4809-4817 (1998).
9. A. Mekis, J.C. Chen, I. Kurland, S.H. Fan, P.R. Villeneuve, and J.D. Joannopoulos, "High Transmission through Sharp Bends in Photonic Crystal Waveguides", *Phys. Rev. Lett.* **77**, 3787-3790 (1996).
10. S.Y. Lin, E. Chow, V. Hietala, P.R. Villeneuve, and J.D. Joannopoulos, "Experimental Demonstration of Guiding and Bending of Electromagnetic Waves in a Photonic Crystal", *Science* **282**, 274-276 (1998).
11. S. Fan, S.G. Johnson, J.D. Joannopoulos, C. Manolatu, and H.A. Haus, "Waveguide branches in photonic crystals", *J. Opt. Soc. Am. B* **18**, 162-165 (2001).
12. S. G. Johnson, C. Manolatu, S. Fan, P. R. Villeneuve, J. D. Joannopoulos, and H. A. Haus, "Elimination of cross talk in waveguide intersections", *Opt. Lett.* **23**, 1855-1857 (1998).
13. S.H. Fan, P.R. Villeneuve, and J.D. Joannopoulos, "Channel drop tunneling through localized states", *Phys. Rev. Lett.* **80**, 960-963 (1998).
14. T. Zijlstra, E. van der Drift, M.J.A. de Dood, E. Snoeks, and A. Polman, "Fabrication of two-dimensional photonic crystal waveguides for 1.5 μm in silicon by deep anisotropic dry etching", *J. Vac. Sci. Technol. B* **17**, 2734-2739 (1999).
15. A. Yariv, Y. Xu, R.K. Lee, and A. Scherer, "Coupled-resonator optical waveguide: a proposal and analysis", *Opt. Lett.* **24**, 711-713 (1999).
16. Y. Xu, R.K. Lee, and A. Yariv, "Propagation and second-harmonic generation of electromagnetic waves in a coupled-resonator optical waveguide", *J. Opt. Soc. Am. B* **17**, 387-400 (2000).
17. M. Bayindir, B. Temelkuran, and E. Ozbay, "Propagation of photons by hopping: A waveguiding mechanism through localized coupled cavities in three-dimensional photonic crystals", *Phys. Rev. B* **61**, R11855-11858 (2000).
18. E. Lidorikis, M.M. Sigalas, E. Economou, and C.M. Soukoulis, "Tight-binding parametrization for photonic band gap materials", *Phys. Rev. Lett.* **81**, 1405-1408 (1998).
19. A.R. McGurn, "Green's-function theory for row and periodic defect arrays in photonic band structures", *Phys. Rev. B* **53**, 7059-7064 (1996).
20. S.F. Mingaleev and Yu.S. Kivshar, "Effective equations for photonic crystal waveguides and circuits", *Opt. Lett.* **27**, 231-233 (2002).
21. F. Delyon, Y.-E. Lévy, and B. Souillard, "Nonperturbative bistability in periodic nonlinear media", *Phys. Rev. Lett.* **57**, 2010-2013 (1986); Q. Li, C.T. Chan, K.M. Ho, and C.M. Soukoulis, "Wave propagation in nonlinear photonic band-gap materials", *Phys. Rev. B* **53**, 15577-15585 (1996); E. Centro and D. Felbacq, "Optical bistability in finite-size nonlinear bidimensional photonic crystals doped by a microcavity", *Phys. Rev. B* **62**, R7683-R7686 (2000).
22. M. Scalora, J.R. Dowling, C.M. Bowden, and M.J. Bloemer, "The photonic band edge optical diode", *J. Appl. Phys.* **76**, 2023-2026 (1994).
23. M.D. Tocci, M.J. Bloemer, M. Scalora, J.P. Dowling, and C.M. Bowden, "Thin-film nonlinear optical diode", *Appl. Phys. Lett.* **66**, 2324-2326 (1995).